

A Method for the Unified Representation of Multispectral Images with Different Number of Bands

Toshio Uchiyama,* Masahiro Yamaguchi, Hideaki Haneishi[▲], and Nagaaki Ohyama

Telecommunication Advancement Organization of Japan, Tokyo, Japan

Satoshi Nambu[▲]

NTT Data Corporation, Tokyo, Japan

We propose a simple but useful method to represent multispectral images captured by multispectral cameras (MSC) with different numbers of bands. When considering accurate color reproduction under an arbitrary illuminant, it is necessary to represent them in a common space with sufficient accuracy of spectral information, estimated from each multispectral image. The principal component analysis (PCA) is useful to reduce the high dimension of the spectral information. However, PCA-based methods may cause both large differences in dynamic range between coefficients of the basis functions derived from the PCA and negative pixel values, therefore, it is not easy to handle or edit coefficient images. To solve the problem, we propose the idea of a virtual multispectral camera (VMSC) that transforms real multispectral images into virtual multispectral images. We design the sensitivities of the VMSC properly, and our unified representation can avoid some disadvantages of conventional PCA-based methods. We experimentally demonstrate the color reproduction accuracy of our method by comparing it with the PCA-based methods, and we show an example of a virtual multispectral image transformed by our method.

Journal of Imaging Science and Technology 48: 120–124 (2004)

Introduction

Recent progress in multispectral imaging technologies has enabled us to reproduce the color of objects accurately under an arbitrary illuminant.¹ This advantage could make it possible to create composites of multispectral images without incongruity, even if those images are captured under different illuminations. We are intending to edit multispectral still images and video as is done with conventional RGB images and video to create attractive video products with accurate color reproduction.

However, there exist many kinds of MSCs that produce multispectral images with different numbers of bands, and there is not yet a simple way of handling them together. Therefore, when considering editing, such as blending two or more videos with different numbers of bands, we need a method to represent them in a common space. In addition, we want a simple representation of the edited result, especially for real-time video processing and display. Colorimetric representation, such as CIE XYZ-values, is well known as a common

space, but it is unusable in the case when capturing and observing illuminations are different. We need to find a method to represent sets of multispectral images in a common space with the sufficient accuracy of spectral information to be estimated from each multispectral image. Hill² also pointed out the same problem in building color reproduction open system architectures, which assume an arbitrary numbers of bands for both input and output devices. In the open system, input multispectral images with a certain number of bands have to be encoded in a generalized form for transportation to output devices.

Concerning efficiency in representation of the spectral information, the principal component analysis (PCA) is useful to reduce the high dimensionality of the spectral information.^{2,3} With this method, all multispectral images are represented as coefficient images of the same set of basis functions. Keusen and Praefcke⁴ introduced a modified version of PCA that is compatible with the conventional tristimulus model. In their method, the first three coefficients represent tristimulus values of a standard color space referred to a standard illuminant. Murakami et al.⁵ proposed weighted Karhunen–Loeve transform (WKLT) which is based on human visual sensitivities and designed to minimize the color difference between the original and the reproduction. Those PCA-based methods theoretically give one of the best results in a sense of minimizing root mean square error. However, there are some disadvantages connected with them. They may cause large differences in dynamic range between coefficients of the basis functions, and also negative pixel values. Therefore, it is

Original manuscript received June 23, 2003

▲ IS&T Member

* uchiyama@akasaka.tao.go.jp

©2004, IS&T—The Society for Imaging Science and Technology

difficult to grasp the meaning of the coefficient images and handling them. In addition, since the basis functions depend on the set of samples, the best set of basis functions for one group might not be good enough for another group. Given any kind of multispectral video as input, it may prove impossible to get perfect PCA basis functions for all.

König et al.⁶ reported significant simulation results by comparing color estimation accuracy using multispectral images from a VMSC (Virtual multispectral camera) using between 6 and sixteen bands. The results suggested the possibility of keeping mean ΔE_{ab} error under 0.5 by using more than 10 bands. In this way, representation of spectral information as output images of a VMSC with such a small number of bands is reasonable for accurate color reproduction. In this article, we propose a simple but useful idea to define a VMSC with a certain number of bands, eight for example, that transforms real multispectral images with different numbers of bands into virtual multispectral images with the same number of bands. Then, the virtual multispectral images are independent from original input devices. We design our VMSC to have equal sensitivities for each band located at equal intervals over the visible range. Our method can avoid the disadvantages of PCA-based methods described above while keeping color reproduction accuracy. We experimentally demonstrate how color reproduction accuracy changes when images with different number of bands are transformed to output images of the defined VMSC. In addition, some experimental results comparing our method with conventional PCA-based methods and an example of a virtual multispectral image transformed by our method are also shown.

Image Model and Unified Representation of Multispectral Images

In this section, we describe the formulation of the image model, and explain the unified representation of multispectral images with different number of bands. Suppose that there exist multiple kinds of MSCs with different number of bands. Let \mathbf{v}_i be a multispectral image captured by the i th camera with N_i bands, and \mathbf{r} be the spectral reflectance of the object represented in an M -dimensional space. Let S_i be an $N_i \times M$ matrix whose row vectors represent the sensitivity of the k th band of the i th camera, and L be an $M \times M$ diagonal matrix whose diagonal elements represent the spectral radiance of the capturing illuminant. We can then write an expression for \mathbf{v}_i in vector representation as follows,

$$\mathbf{v}_i = F_i \mathbf{r}, \quad (1)$$

where $F_i (= S_i L)$ is a linear system matrix with size of $N_i \times M$. Note that each multispectral image \mathbf{v}_i has a different number of bands N_i , while the spectral reflectance \mathbf{r} is represented in the same M -dimensional space. Our problem is to find a method to represent these \mathbf{v}_i with different number of bands in a common space to handle them together. We call this kind of representation that has only one form for all multispectral images as “unified representation”.

We can get the estimated reflectance from each \mathbf{v}_i by using Wiener estimation^{7,8}:

$$\begin{aligned} \hat{\mathbf{r}}_i &= G_i \mathbf{v}_i, \\ G_i &= R_i F_i^t (F_i R_i F_i^t)^{-1} \end{aligned} \quad (2)$$

where, R_i is a correlation matrix of \mathbf{r} , which is related to a priori knowledge about the reflectance \mathbf{r} of objects in the image. G_i is a matrix with size of $M \times N_i$.

Since $\hat{\mathbf{r}}_i$ in Eq. (2) is represented in the same dimensional space for all i , this could be considered as one of the unified representations we demand. However, $\hat{\mathbf{r}}_i$ use in general a so high dimensional space to approximate the continuous value of the spectral reflectance, which is not appropriate for practical applications in the sense of amount of data. Therefore, we have to encode $\hat{\mathbf{r}}_i$ to reduce amounts of data. At that time, we need to concern about efficiency, accuracy and usefulness of this unified representation.

Virtual Multispectral Camera

Before explaining our idea and defining a unified representation of multispectral images, we recall PCA-based methods as a comparison. By using a PCA method basically, the estimated spectral reflectance $\hat{\mathbf{r}}_i$ can be encoded into a coefficient image \mathbf{x}_i in a lower dimensional space. This \mathbf{x}_i theoretically gives one of the best representations in the sense of minimizing square error between the original $\hat{\mathbf{r}}_i$ and the one that is recalculated from \mathbf{x}_i .

However, they may cause large differences in dynamic range between coefficients of basis functions, and also negative pixel values. Therefore, it is difficult to grasp the meaning of the coefficient images and handling them. In addition, since the basis functions depend on the set of samples, the best set of basis functions for one group might not be good enough for another group. Considering any given kind of multispectral video as input, it may be impossible to get perfect PCA basis functions for all inputs.

Our method, on the other hand, can avoid these disadvantages of PCA-based methods described above. The idea relies on the simulation results reported by König et al.,⁶ which suggested the reliability of a multispectral image from a VMSC with a relative numbers of bands to reproduce accurate color. A VMSC here means a virtual and unreal device with virtual spectral sensitivities that can transform spectral radiant distribution into a VMSC response. We utilize this VMSC to represent the estimated spectral reflectance $\hat{\mathbf{r}}_i$. We design this camera properly to have equal sensitivities for each band located at equal intervals over visible range of wavelength in order to be independent from input data, and not to produce negative pixel values. Since the VMSC is physically defined, it is easy to grasp and handle the multispectral image from the VMSC. Further details are explained below. First of all, using Eqs. (1) and (2), we can transform both a real multispectral image \mathbf{v}_i with arbitrary number of bands and the estimated spectral reflectance $\hat{\mathbf{r}}_i$ to a virtual multispectral image $\tilde{\mathbf{v}}_i$ as

$$\tilde{\mathbf{v}}_i = F_\phi \hat{\mathbf{r}}_i = F_\phi G_i \mathbf{v}_i \quad (3)$$

where F_ϕ is a matrix with size of $N_\phi \times M$ that defines the properties of this transformation. Equation (3) defines our VMSC. Since there are no differences between the form of $\tilde{\mathbf{v}}_i$ and \mathbf{v}_i , we can estimate spectral reflectance again from $\tilde{\mathbf{v}}_i$ using Eq. (2) as

$$\check{\mathbf{r}}_i = G_\phi \tilde{\mathbf{v}}_i, \quad (4)$$

where G_ϕ is a matrix that corresponds to G_i in Eq. (2), but that is independent from the linear system matrix F_i . In addition, any applications for real multi-

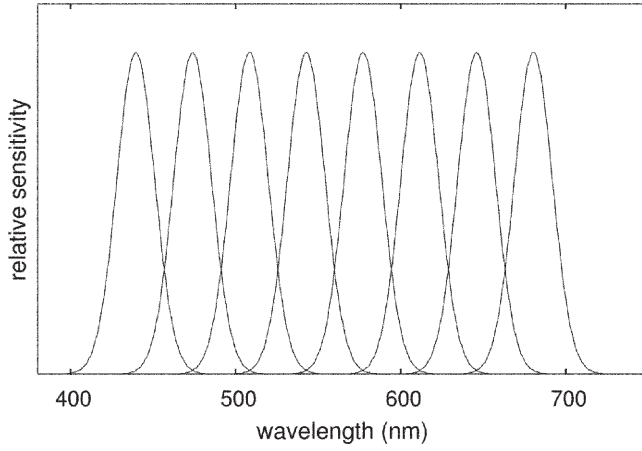


Figure 1. An example of spectral sensitivities of a VMSC

spectral images \mathbf{v}_i can be applied to virtual multispectral images $\hat{\mathbf{v}}_i$.

Now, let us show the design of the matrix F_ϕ , which is the key of our method. We should design F_ϕ properly in the sense of efficiency, accuracy and usefulness. We take a different approach from PCA-based methods to avoid the explained disadvantages. In order to cover all kind of objects to be captured, we design our VMSC to be not optimized for particular sample data. To realize this, we used Gaussian curves to define the k th spectral sensitivity as

$$\mathbf{F}_\phi(k, \lambda) = \frac{1}{\sqrt{2\pi}\sigma} \exp\left\{-\frac{\{\lambda - (\mu_0 + k\Delta\mu)\}^2}{2\sigma^2}\right\} \quad (5)$$

where λ is wavelength and σ , μ_0 , $\Delta\mu$ are constants, the capturing illuminant is represented by a unit matrix. Since all elements in matrix F_ϕ are positive values, this does not cause negative pixel values.

An example of spectral sensitivities of an eight band VMSC of Eq. (5) is shown in Fig. 1. Next, we confirm the color reproduction accuracy of our method through experiments.

Experiments

We evaluated the color reproduction accuracy of our method by simulation. The object data we used for the simulations were sets of spectral reflectances of the Gretag Macbeth Color Checker measured by a spectroradiometer (Topcon SR-2), the natural objects measured by Vrhel, Gershon and Iwan,³ and flowers, leaves, and paints from the SOCS (Standard Object Colour Spectra database for color reproduction evaluation).⁹ As real input devices, we used spectral sensitivities of real three- and six-band multispectral video cameras and a sixteen band multispectral still camera.¹

In our simulation, the illuminant for image capture was CIE D65, and the ones used for color reproduction were CIE D65, CIE A, CoolWhite, and TL84. We used Eq. (5) as definition of our VMSC with constant values σ , μ_0 , and $\Delta\mu$ adjusted to cover the range between 380 nm to 780 nm at equal intervals. The numbers of VMSC bands N_ϕ were 4, 6, 8, and 10. Actually, we selected them as follows. As Eq. (5) shows, center wavelength of k -th band of a VMSC with N_ϕ bands can be written as

$$\mu = \mu_0 + k\Delta\mu, (k = 1, \dots, N_\phi), \quad (6)$$

and we selected μ_0 and $\Delta\mu$ by

$$\begin{aligned} \mu_0 &= 380(\text{nm}) + \Delta_1, \\ \mu_0 + (N_\phi + 1)\Delta\mu &= 780(\text{nm}) - \Delta_2, \end{aligned} \quad (7)$$

where Δ_1 and Δ_2 are offsets to increase spectral resolution of VMSC's sensitivities. We experimentally selected Δ_1 and Δ_2 as 25 nm and 65 nm respectively. Then we chose σ by $\sigma = 3\Delta\mu$. As seen in Eqs. (1) to (4), there are three different types of reflectances, which are

1. The authentic original spectral reflectance \mathbf{r} of objects.
2. The spectral reflectance $\hat{\mathbf{r}}_i$ estimated from a real multispectral image.
3. The spectral reflectance $\check{\mathbf{r}}_i$ re-estimated from a virtual multispectral image whose input is $\hat{\mathbf{r}}_i$.

We evaluated the differences of the re-estimated reflectance $\check{\mathbf{r}}_i$ against the original reflectance \mathbf{r} to check the total system performance. Since there already exist estimation errors in the estimated reflectance $\hat{\mathbf{r}}_i$, differences of the re-estimated reflectance $\check{\mathbf{r}}_i$ against the estimated reflectance $\hat{\mathbf{r}}_i$ are also confirmed. For evaluation of the color reproduction accuracy from the re-estimated spectral reflectance, we computed the root mean square errors (RMSE) between the re-estimated and the estimated reflectances, and we also computed the ΔE_{ab} average color differences of the reproductions under the four illuminants.

In Wiener estimation (Eq. (2)), we used the correlation matrix R^r which is modeled as a first order Markov process covariance matrix⁸ of the form

$$\mathbf{R}^r = \begin{pmatrix} 1 & \rho & \rho^2 & \dots & \rho^{M-1} \\ \rho & 1 & \rho & \dots & \rho^{M-2} \\ \rho^2 & \rho & 1 & \dots & \dots \\ \dots & \dots & \dots & \dots & \dots \\ \rho^{M-1} & \rho^{M-2} & \dots & \dots & 1 \end{pmatrix}, \quad (8)$$

where $0 \leq \rho \leq 1$ is the adjacent element correlation factor and we selected $\rho = 0.999$ for this experiment.

We compared our method with two kinds of PCA-based methods, which are a normal PCA method and WKLT.⁵ The reflectance that is recalculated from the coefficient image of these PCA-based methods corresponds to the re-estimated reflectance of our method. For ease of expression, we will use the term re-estimate for both reflectances. Since we want to represent arbitrary multispectral images in a common space, the basis functions of the PCA should be also common. Therefore, we derived a set of basis functions from the estimated reflectances of the mixed set of all kinds of input data groups. In addition, we also derived sets of basis functions from each individual input data group for reference. We indicated them by “(mix)” and “(ind)” respectively in Figs. 2 to 6.

Experiment 1

We used the sixteen band real MSC and an eight band VMSC or eight dimensional PCA-based methods. The number of VMSC bands N_ϕ was chosen by the assumption that the maximum and average color differences of ΔE_{ab} had to be fewer than 2.0 and 0.5 respectively for both the Color Checker and natural objects sets. We compared the color reproduction differences for various sets of objects. A comparison of average RMSEs for the re-estimated reflectance against the original reflectance is

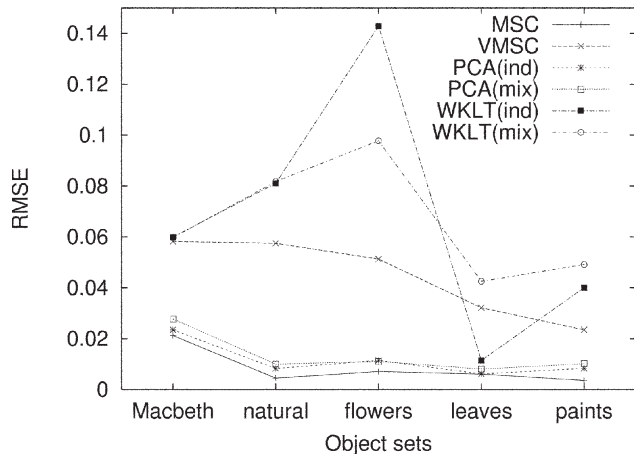


Figure 2. Average RMSEs for the re-estimated against the original reflectance about various object sets.

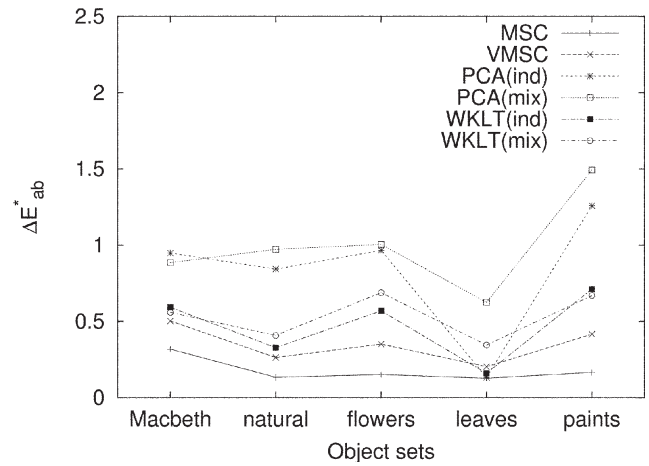


Figure 3. ΔE_{ab}^* average color difference for various object sets.

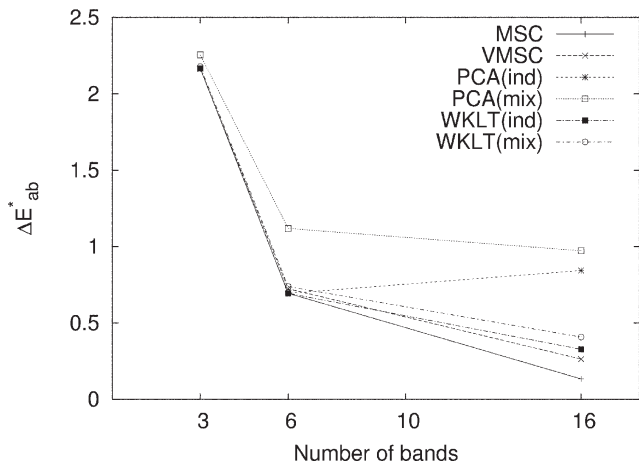


Figure 4. ΔE_{ab}^* average color difference versus the number of MSC bands (against the original reflectance).

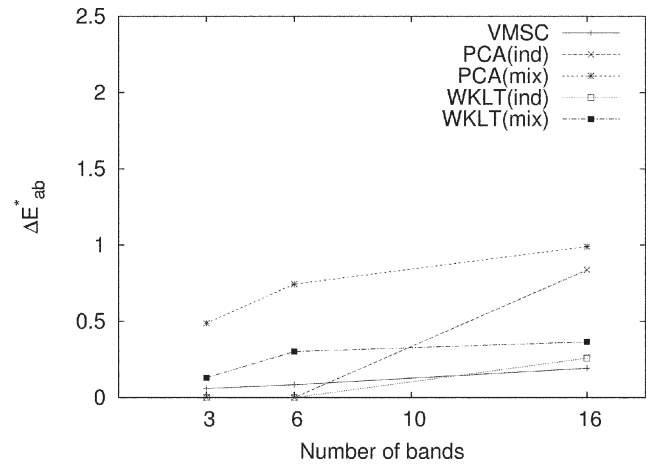


Figure 5. ΔE_{ab}^* average color difference versus the number of MSC bands (against the estimated reflectance).

shown in Fig. 2, and a comparison of color differences is shown in Fig. 3. In the figures, “MSC” means the estimated reflectance from the real MSC, that is shown for reference to see how much the re-estimated reflectance of each method lost color information from the estimated reflectance. PCA(mix) and PCA(ind) gave the best results for the average RMSEs in Fig. 2, but results were quite worse in color differences in Fig. 3. To get better results of color reproduction, human visual sensitivities have to be considered. As it was expected, WKLT(mix) and WKLT(ind) that are based on human visual sensitivities⁵ gave better results on measured color differences than PCAs. However, our method, which is not optimized for the sample set, gave the best result of all the methods except on the leaves set. One reason for this may be that our method used a priori knowledge about reflectance, which is the smoothness assumption as defined in Eq. (8), and the object data for the experiments actually presented smooth reflectance.

Experiment 2

We used the eight band VMSC, and the object sets of the Color Checker and the natural objects. We changed the number of input real MSC bands to see the influence to the color differences. A comparison of the re-

sults for the computed average color differences of the re-estimated reflectance using natural objects against the original reflectance and the estimated reflectance respectively are shown in Figs. 4 and 5.

In Figs. 4 and 5, the performance of our method was equal or better than the other four methods for almost all cases. The color differences of the recalculated reflectance against the estimated reflectance of PCA(ind) and WKLT(ind) for three and six band MSCs are zero in Fig. 5, because the estimated reflectance \hat{r}_i represented in Eq. (2) has the same or less rank than the number of its MSC bands and it can be represented by higher dimensional PCA without error.

Experiment 3

We used the sixteen band real MSC, and the object sets of Color Checker and the natural objects. We changed the number of bands of the VMSC and the dimensions of the PCA-based method to see the effect on the color differences. A comparison of the results about the computed average color differences of the re-estimated reflectance against the original reflectance using natural objects is shown in Fig. 6. The performance of our method was equal or better than the other four methods in higher than six-dimensional spaces, but it

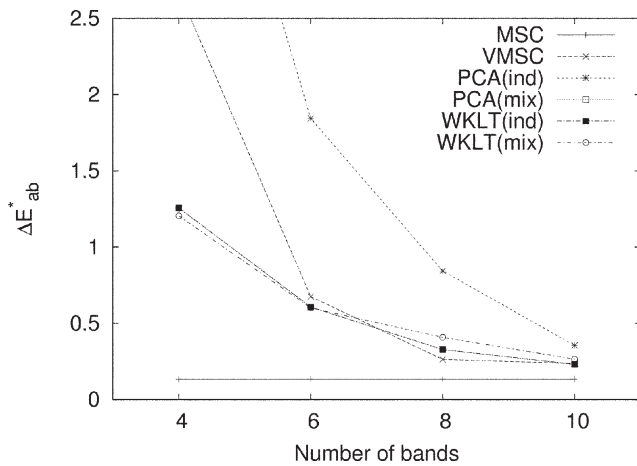


Figure 6. ΔE_{ab}^* average color difference vs. the number of VMSC bands or PCA dimensions

was worse than WKLT(mix) and WKLT(ind) in four dimensional space. This means that our method is effective in a higher dimensional space where the total color reproduction accuracy is high.

Finally we show an example of a virtual multispectral image (the Gretag Macbeth Color Checker) transformed by our method in Fig. 7. The original multispectral image is captured by the camera with sixteen bands under Xenon lamp illumination. As shown in Fig. 7, each band image presents the reflectance of the corresponding wavelength of the virtual multispectral camera (see Fig. 1). Since the VMSC is physically defined, it is easy to grasp and handle these data. In addition we checked the color differences about all the 24 patches in the Gretag Macbeth Color Checker of Fig. 7. The average RMSEs of estimated reflectances from MSC $\hat{\mathbf{r}}$ and re-estimated reflectance from VMSC $\hat{\mathbf{r}}$ against the original data are 0.047 and 0.062. The average color differences ΔE_{ab}^* of estimated from MSC and re-estimated from VMSC under the capture illumination are 0.80 and 0.83. The average color differences ΔE_{ab}^* of estimated from MSC and re-estimated from VMSC under the four illuminations (CIE D65, CIE A, CoolWhite, TL84) are 0.87 and 0.98. Thus, the virtual

multispectral image may preserve enough spectral information for accurate color reproduction.

Conclusion

We have demonstrated the color reproduction accuracy of our method by means of experiments. Since the VMSC is physically defined, it is easy to grasp and handle the virtual multispectral imagery. According to the results of the experiments, our method also shows the same or better accuracy in color reproduction compared with conventional PCA-based methods. This result also suggests the effectiveness of our method for representing multispectral images with different numbers of bands into a unified common space. We propose that the reason for this result was the smoothness assumption of reflectance as we intend to confirm in future work. \blacktriangle

Acknowledgment. We would like to thank all members of Natural Vision project for a helpful discussion.

References

1. M. Yamaguchi, T. Teraji, K. Ohsawa, T. Uchiyama, H. Motomura, Y. Murakami, and N. Ohya, Color image reproduction based on the multispectral and multiprimary imaging: Experimental evaluation, *Proc. SPIE* **4663**, 15–26 (2002).
2. B. Hill, Aspects of total multispectral image reproduction systems, *Proc. Int. Symposium on High Accurate Color Reproduction and Multispectral Imaging*, 2000, pp. 67–78.
3. M. J. Vrhel, R. Greshon, L. S. Iwan, Measurement and analysis of object reflectance spectra, *Color Res. Appl.* **19**, 4–9, (1994).
4. T. Keusen, Multispectral color system with an encoding format compatible with the conventional tristimulus model, *J. Imaging Sci. Technol.* **40**:6, 510–515 (1996).
5. Y. Murakami, H. Manabe, T. Obi, M. Yamaguchi, and N. Ohya, Multispectral image compression for color reproduction: Weighted KLT and adaptive quantization based on visual color perception, *Proc. IS&T/SID 2nd Color Imaging Conference*, IS&T, Springfield, VA, 2001, pp. 68–72.
6. F. König and W. Praefcke, A multispectral scanner, *Proc. IS&T/SID 2nd Color Imaging Conference*, IS&T, Springfield, VA, 1998, p. 63.
7. H. Haneishi, T. Hasegawa, A. Hosoi, Y. Yokoyama, N. Tsumura, and Y. Miyake, System design for accurately estimating the spectral reflectance of art paintings, *J. Opt. Soc. Amer.* **39**, 6621–6632 (2000).
8. W. K. Pratt and C. E. Mancill, Spectral estimation techniques for the spectral calibration of a color image scanner, *Appl. Opt.* **15**, 73–75 (1976).
9. J. Tajima, M. Tsukada, Y. Miyake, H. Haneishi, N. Tsumura, M. Nakajima, Y. Azuma, T. Iga, M. Inui, N. Ohta, N. Ojima, and S. Sanada, Development and standardization of a spectral characteristics data base for evaluating color reproduction in image input devices, *Proc. SPIE*, **3409**, 42–50 (1998).

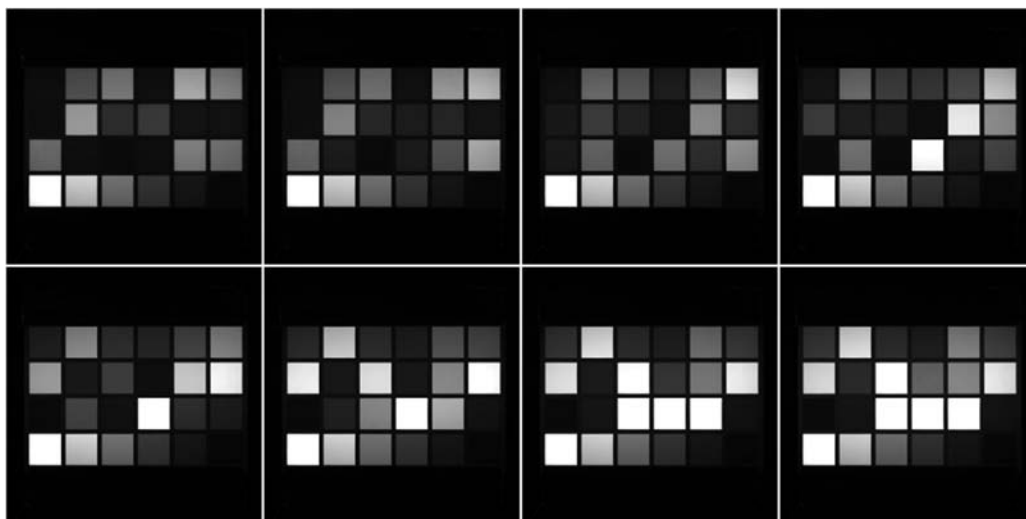


Figure 7. An example of virtual multispectral image (the Gretag Macbeth Color Checker) transformed by our method. A band image of the lowest wavelength is at top-left and wavelength is increasing according to reading order.